



## Hydrolytic hydrogenation of hemicellulose over metal modified mesoporous catalyst

Bright T. Kusema<sup>a</sup>, Laura Faba<sup>b</sup>, Narendra Kumar<sup>a</sup>, Päivi Mäki-Arvela<sup>a</sup>, Eva Díaz<sup>b</sup>, Salvador Ordóñez<sup>b</sup>, Tapio Salmi<sup>a</sup>, Dmitry Yu. Murzin<sup>a,\*</sup>

<sup>a</sup> Laboratory of Industrial Chemistry and Reaction Engineering, Process Chemistry Centre, Department of Chemical Engineering, Åbo Akademi University, FI-20500 Åbo/Turku, Finland

<sup>b</sup> Department of Chemical Engineering and Environmental Technology, Faculty of Chemistry, University of Oviedo, 33006 Oviedo, Spain

### ARTICLE INFO

#### Article history:

Received 30 September 2011

Received in revised form 7 January 2012

Accepted 12 February 2012

Available online 8 March 2012

#### Keywords:

Hemicellulose  
Arabinogalactan  
Hydrolysis  
Hydrogenation  
Dehydration  
Heterogeneous catalysts  
Ruthenium  
MCM-48

### ABSTRACT

The hydrolytic hydrogenation of hemicellulose arabinogalactan, into sugars, sugar alcohols and furfurals was carried out in a batch reactor using modified mesoporous MCM-48 material incorporated with ruthenium metal into the framework. The bi-functional catalytic materials, MCM-48 and Ru-MCM-48 were synthesized, characterized and investigated in the title reaction at total pressure of 20 bar hydrogen, using an initial arabinogalactan concentration of 0.4 wt%, at 458 K. The transformation of the hemicellulose consists of arabinogalactan hydrolysis to the monosaccharides, L-arabinose and D-galactose followed by the subsequent hydrogenation to sugar alcohols, arabitol and galactitol or dehydration of the monomers to furfural and 5-hydroxymethylfurfural. The yields of the main products, i.e. sugars, sugar alcohols and furfurals were varied depending on the strength of the acid sites and the presence of metal in the structure of the ruthenium modified catalyst. Ru-MCM-48 displayed high catalytic activity and the sugar alcohols were obtained selectively from the hemicellulose. The catalytic performance of the mesoporous MCM-48 catalysts with respect to the catalyst structure, acidity and presence of the metal was evaluated.

© 2012 Elsevier B.V. All rights reserved.

### 1. Introduction

The catalytic transformation of biomass based feedstocks into chemicals, materials and fuels has attracted great attention in recent years [1,2]. The processes involved in the upgrading of these renewable feedstocks should integrate the principles of green chemistry and green engineering, and low environmental impact technologies for the sustainable production of the high value chemicals. The application of catalysis and innovative process design plays an important role in the development of this technology. In addition, it is essential to study and analyze ethical, political and economical concerns related with the renewable, consistent and regular supply of the feedstock. Forest based biorefinery uses non-food woody biomass feedstocks which is made up of lignocellulose. Lignocellulosic material consists of three primary fractions; cellulose, hemicellulose and lignin. Hemicelluloses are hetero-polymers made up of pentoses and hexoses. These macro molecules are the second most abundant polysaccharides in nature after cellulose, accounting for 20–30% of lignocellulosic biomass [3]. Hemicelluloses such as arabinogalactans appear in large quantities in larch species, such as *larix sibirica*. The structural basis of arabinogalactan

is a backbone of  $\beta$ -D-galactopyranose residues that are predominantly (1  $\rightarrow$  3)-linked and branched with D-galactopyranose and L-arabinofuranose side chains [4]. The average molar ratio of galactose:arabinose in arabinogalactan is about 5.6:1 and the molar mass is 20,000–100,000 g/mol. The extraction of arabinogalactan can easily be achieved in water at moderate conditions on an industrial scale [5,6]. Therefore, it has a great potential to serve as a sustainable feedstock for valuable chemicals.

The hydrolysis of cellulose and hemicelluloses is considered as the most important entry point into the biorefinery scheme based on carbohydrates [7]. During acid hydrolysis of the polysaccharides, the glycosidic bonds between the sugar units are cleaved to form simple monosaccharides. Hydrolysis of arabinogalactan to produce L-arabinose and D-galactose over homogeneous and heterogeneous catalysts without further degradation of the monomers has been recently reported [8,9]. The acid hydrolysis of hemicelluloses is influenced by their structures, the conformation of the individual sugar units and the acidic medium. Due to their branched and non-crystalline structures, hemicelluloses are easier to hydrolyze to their monomeric sugar components than cellulose [10]. Although the hydrolysis of the hemicelluloses and cellulose can be performed in high yields by homogeneous acid catalysts, they however, have disadvantages such as the treatment of waste generated and corrosion of the equipments. A lot of interest has been put on the one-pot catalytic transformation of cellulose and hemicellulose using

\* Corresponding author. Tel.: +358 2 215 4985; fax: +358 2 215 4479.  
E-mail address: [dmurzin@abo.fi](mailto:dmurzin@abo.fi) (D.Yu. Murzin).

heterogeneous catalysts in the aqueous media [11–13]. The conversion of cellulose as well as hemicelluloses, such as arabinan and xylan, to sugar alcohols over various catalysts and supported metals such as ruthenium and platinum was reported in Ref. [13]. The reaction involves the hydrolysis of the lignocellulosic biomass into sugars followed by the hydrogenation of the sugars to sugar alcohols and the dehydration into furfurals.

Hydrolytic hydrogenation is an attractive alternative since it converts the hemicellulose into sugars, sugar alcohols and furfurals in a single step process using only water as a solvent in the presence of hydrogen. The catalysts used for these reactions should bear a large enough porous structure in order to avoid pore blockage and mass transfer limitations as well as regular acid sites distribution. Since reduction is one of the main desired reaction steps, the presence of active metal functionalities is of a necessity for accomplishing it. The bi-functional catalytic strategy bearing both acid and metal sites is therefore an elegant route for the transformation of hemicelluloses into valuable chemicals. The first step in the hydrolytic hydrogenation of arabinogalactan is the hydrolysis over the acidic support material into monosaccharides *L*-arabinose and *D*-galactose. Thereafter, the hydrogenation of the free sugars takes place on the active metal sites, ruthenium or platinum, of the catalyst into polyols. Due to the acidic nature of the catalyst, dehydration of the sugars also occurs to produce furfurals. A good balance between the two catalytic functions of the catalyst is a necessity for the overall productivity of the desired products. The sugar alcohols have many applications such as low caloric, non-carcinogenic sweeteners in the food and pharmaceutical industries while furan compounds can be used as industrial solvents, fuel additives and chemical intermediates [2,14–16].

In the present work, the hydrolytic hydrogenation of arabinogalactan over MCM-48 and ruthenium metal modified Ru-MCM-48 materials was investigated. MCM-48 is an aluminosilicate ordered mesoporous molecular sieve first introduced by the researchers at Mobil Corporation [17,18]. The ordered mesoporous MCM-48 has a high surface area, large pore structure of diameter 27.8 Å and three dimensional systems beneficial for diffusion of large molecules [19,20]. Furthermore, solid acid catalysts with Brønsted acidity analogous to HCl and H<sub>2</sub>SO<sub>4</sub> are known to catalyze the hydrolysis of hemicelluloses. The choice of ruthenium supported catalysts is based on the reported superior activity and selectivity for sugar hydrogenation to sugar alcohols [21]. The incorporation of ruthenium into the microporous and mesoporous molecular sieves and the preparation of ruthenium metal clusters for different catalytic applications have been reported in the literature [22–24]. The metal modification of the mesoporous materials provides a possibility for the preparation of catalysts with unique properties. The catalytic performance of the mesoporous MCM-48 catalysts with respect to the catalyst structure, acidity and presence of the metal was evaluated for the hydrolytic hydrogenation of arabinogalactan.

## 2. Experimental

### 2.1. Catalyst preparation

The synthesis of Al-MCM-48 ordered mesoporous material was carried out according to the procedures described in Ref. [17,20] with some modifications. NaOH and cetyl trimethyl ammonium chloride (CTMACl) were added to deionized water. Aluminum isopropoxide (AIP) was added to the solution and stirred for 15 min to allow the hydrolysis of AIP. Finally, tetraethyl orthosilicate (TEOS) was added and stirred in an open vessel at room temperature for 1 h to achieve complete hydrolysis of TEOS. The pH of the mixture was measured. The gel was transferred into a 300 ml autoclave, thereafter the synthesis was carried out at 373 K for 75 h. Na-MCM-48

ordered mesoporous material was ion-exchanged with an ammonium chloride solution for 48 h, washed with deionized water, dried at 373 K and calcined at 773 K to obtain H-MCM-48 catalyst.

Ru-MCM-48 catalyst was prepared by ion exchange with an aqueous solution of ruthenium chloride (Ru/Cl<sub>3</sub>) (Fluka). The exchange procedure was performed at 343 K for 24 h, according to previously optimized processes for obtaining the desired metal loading [12]. The catalyst was dried at 373 K and calcined at 623 K after the ruthenium incorporation. Prior to the catalytic tests, the ruthenium metal modified catalyst was activated at 573 K for 2 h under flowing hydrogen gas. In order to get a narrow particle size range of the catalysts, pellets of the powder were first pressed and thereafter crushed and sieved to the particle size range below 63 μm.

### 2.2. Catalyst characterization

The metal loading of the catalysts was determined by ICP-OES using a SPECTRO-CIROSCCD ICP-spectrometer. Approximately 50 mg of the sample was inserted into a teflon bomb; 4 ml of HF, 1 ml of HCl and 0.5 ml of HNO<sub>3</sub> were added. The sample was dissolved in a microwave oven, and diluted with deionized water and analyzed in the spectrometer.

The specific surface area of the fresh and spent catalysts was measured by the nitrogen adsorption method (Sorptometer 1900, Carlo Erba Instruments). The catalysts were out-gassed at 423 K prior to the measurement and the BET equation was used to calculate the specific surface area.

The metal dispersion of the catalyst was determined from the amount of chemisorbed CO by a pulse method. The analysis was carried out using a Micromeritics TPD/TPR 2910 AutoChem instrument. About 150 mg of the sample was inserted into a quartz U-tube and was reduced with H<sub>2</sub> stream (AGA, 99.999%, 20 ml/min). A ramp rate of 5 K/min was applied and the temperature was linearly raised to the final temperature 623 K, thereafter it was held for 120 min. Then, the sample was cooled to 313 K under flowing He (AGA, 99.999%) and the analysis started once the baseline was stable. The CO (AGA, 10% in He) was introduced and the pulses were repeated until complete saturation. The stoichiometry of CO to ruthenium was assumed to be 0.6 [25,26].

The acidity of the synthesized mesoporous materials was measured by infrared spectroscopy (ATI Mattson FTIR) using pyridine (≥99.5%, a.r.) as a probe molecule for qualitative and quantitative determination of both the Brønsted (BAS) and Lewis acid sites (LAS). The FTIR spectrometer was equipped with an in situ cell containing ZnSe windows. The samples were pressed into thin self-supported wafers (weight 15–20 mg and radius 0.65 cm). Pyridine was first adsorbed for 30 min at 373 K and then desorbed by evacuation at different temperatures (523 K, 623 K and 723 K) to obtain a distribution of acid site strengths. All spectra were recorded under vacuum at 373 K with a spectral resolution equal to 2 cm<sup>-1</sup>. Spectral bands at 1545 and 1450 cm<sup>-1</sup> were used to identify the BAS and LAS, respectively. The amounts of BAS and LAS were calculated from the intensities of corresponding spectral bands using the molar extinction coefficients reported in Ref. [27].

X-ray powder diffractometer (Philips PW 1820) was applied to study the structure and phase purity of MCM-48 mesoporous materials, working with the Cu Kα line (λ = 0.154 nm) in the 2θ range of 5–85° at a scanning rate of 2θ of 2°/min. The morphology of the catalytic materials was investigated by scanning electron microscope (SEM). The analysis was conducted by a LEO Gemini 1530 with a Thermo Scientific UltraDry Silicon Drift Detector. Analysis of the carbon and coke deposits on the spent catalysts was performed by temperature programmed oxidation (TPO) in a Micromeritics TPD/TPR 2900. After the pretreatment of 10 mg with He at 723 K for 2 h, the samples were exposed to O<sub>2</sub> stream while the temperature

**Table 1**  
Specific surface area and metal loading of the tested catalysts.

Catalyst	Specific surface area (m <sup>2</sup> /g)	Pore volume (cm <sup>3</sup> /g)	Metal loading (wt%)	Crystallite size (nm)	
				Chemisorption	XRD
MCM-48	718	0.72	–	–	–
Ru–MCM-48	821	0.29	5	14	16

was increased at 5 K/min from 293 K to 873 K. The evolutions of CO and CO<sub>2</sub> signals were monitored by mass spectroscopy.

### 2.3. Hydrolytic hydrogenation experiments

The hydrolytic hydrogenation experiments were performed in a 300 ml Parr autoclave connected to a pre-reactor with a 200 ml volume. The autoclave was provided with a 1 μm filtered sampling outlet, which prevented the small catalyst particles from passing through it. The temperature was measured with a thermocouple and controlled automatically (Brooks Instrument). 600 mg of arabinogalactan was dissolved in 150 ml of deionized water and loaded to the pre-reactor. 300 mg of the catalyst with a particle size below 63 μm was loaded into the reactor. The amount of the catalyst loading was chosen on the basis of the quantity used in the previous study on the hydrolytic hydrogenation of cellulose [12], in order to facilitate a direct comparison between the hydrolytic hydrogenation of cellulose and hemicelluloses under similar reaction conditions. 20 bar of hydrogen pressure was applied and the solution was heated to 458 K. The stirring rate was 1145 rpm to minimize external diffusion affecting activity measurements. When the reactor had reached the desired temperature, stirring was applied and the arabinogalactan solution from the pre-reactor was fed into the reactor. This was considered as the initial reaction time. Liquid samples were periodically withdrawn at different times for analysis.

### 2.4. Product analysis

The liquid phase samples from the reaction mixture were quantitatively analyzed by HPLC. The HPX-87C column was connected to a refractive index (RI) detector and the mobile phase of diluted calcium sulfate solution CaSO<sub>4</sub> with a concentration of 1.2 mM was used. The flow rate was 0.4 ml/min and the temperature was set to 353 K. 0.005 M sulfuric acid solution H<sub>2</sub>SO<sub>4</sub> was used as a mobile phase in the Aminex cation H<sup>+</sup> column. The eluent flow rate was 0.5 ml/min and the temperature was set to 338 K. The samples were injected into the HPLC directly after the experiments without any pretreatment. Using this technique, the evolution of the concentration of the sugars, furan compounds and sugar alcohols was monitored with respect to the reaction time. The product yields were rather conventionally defined as the ratio of the actual concentration of the desired product per theoretical concentration of the compounds present in the liquid phase. Although the compounds, derived from arabinose and galactose, were separately identified, the results have been presented by grouping the classes of compounds indicated in the respective figures.

The samples were also analyzed by GC–MS equipped with an HP-1 column. Prior to GC–MS analysis, the samples were silylated by addition of 100 μl of pyridine (Fluka, 99%), 200 μl of hexamethyldisilazane (Fluka, 98%), and 100 μl of chloromethylsilane (Fluka, 98%) [28].

The total organic compound (TOC–V CSN, Shimadzu) analysis was conducted to determine the amount of total organic carbon dissolved in the liquid phase. The pH of the reaction mixture was also measured at the end of the experiments.

Carbon mass balance was calculated in order to verify the significance of the results, i.e. if there are considerable amount

of by-products in the gas phase (not analyzed). Therefore, mass balance was calculated considering the concentration of sugars, polyols, furfurals and low molecular weight compounds analyzed by HPLC. The carbon and coke which might be deposited over the catalyst surface was also determined by TPO analysis.

## 3. Results and discussions

### 3.1. Catalyst characterization

The specific surface area and Ru metal loadings of the catalytic materials are shown in Table 1. The ordered mesoporous MCM-48 displayed a high specific surface area of the support material. The large pore materials typically have surface areas above 700 m<sup>2</sup>/g [17]. Generally, a decrease in the specific surface area of the catalytic materials after the incorporation of the active metal is noticed, possibly due to the partial blocking of some of the pores. However, the specific surface area of the metal modified 5 wt% Ru–MCM-48 exhibited an enhancement in the specific surface area. This may be attributed to the formation of additional micropores at the expense of the mesopores and the incorporated metal during calcination of the ruthenium modified Ru–MCM-48. The ruthenium metal loading of the catalyst was determined by ICP-OES, obtaining a 5 wt% Ru–MCM-48, which is in good agreement with the nominal loading.

The average metal crystallite size of the Ru–MCM-48 catalytic material measured by CO chemisorption was 14 nm. The crystalline structure of the ruthenium metal modified catalysts studied in this work was also analyzed by XRD and the pattern obtained is shown in Fig. 1. A loss of crystallinity was observed compared with the XRD profiles which corresponds with the original proton form reported in the literature [29,30], especially noticeable in the 2θ between 0° and 20°. Consequently, the main peaks observed are related with different crystalline phases of the active metal. In the ruthenium modified catalyst, these peaks had their maxima at 2θ = 28°, 35° and 54.4°. The width of these peaks can be related with the average crystallite size through the Scherrer equation, resulting in values analogous with the results obtained by CO chemisorption (Table 1).

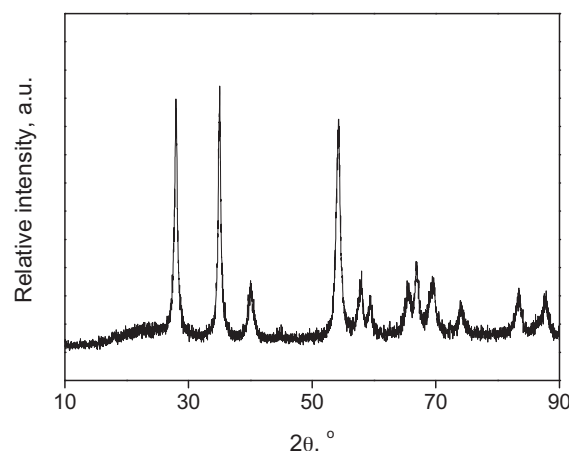


**Fig. 1.** XRD pattern of 5 wt% Ru–MCM-48.

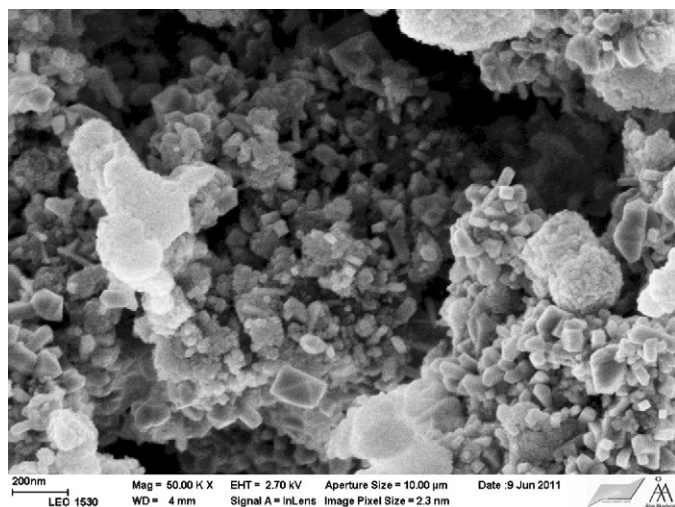


Fig. 2. Scanning electron micrograph of 5 wt% Ru-MCM-48.

The morphology and surface texture of the mesoporous material was investigated by SEM and the micrograph of the ruthenium metal modified Ru-MCM-48 material is shown in Fig. 2. Micrographs obtained of MCM-48 and Ru-MCM-48 showed the typical faceted morphology of the MCM materials [31], retaining the cubic-type ordering with the fully developed crystals.

The acidity of MCM-48 as well as the ruthenium modified Ru-MCM-48 was determined by FTIR using pyridine as a probe molecule and the results are shown in Table 2. The adsorption and desorption of pyridine followed by FTIR spectroscopy at different temperatures enables the BAS to be distinguished from the LAS and to quantitatively determine their concentrations. The presence of the metal in the zeolites and mesoporous materials is known to affect the acidic properties of the support materials [32]. When MCM-48 was modified with ruthenium, the total concentration and strength of the acid sites diminished. The same observations were reported in [32] for a number of metal catalysts supported on zeolite and mesoporous materials. In the current work the medium and strong acid sites of both the BAS and LAS which retain pyridine at 623 and 723 K, respectively, decreased when ruthenium was incorporated in MCM-48. It can be inferred that the observed changes in the distribution of the acid sites and strengths are a result of the interactions between the ruthenium metal crystallites and the support material in line to what was reported in the literature for similar catalytic systems [32]. Therefore, the resulting metal modified catalyst show lower total concentration of BAS and LAS, and strength distribution shifted to weaker interactions.

The specific surface area of the spent catalysts was investigated to verify if there was a change in the structure of the catalytic materials after the experiments. The comparison of the fresh and the spent catalysts revealed that the specific surface area of the mesoporous materials decreased. It was found that the specific surface area of the fresh 5 wt% Ru-MCM-48 was 821 m<sup>2</sup>/g whereas for the spent catalyst it was 240 m<sup>2</sup>/g. The same trend was also observed for the specific pore volume decreasing from 0.29 cm<sup>3</sup>/g to 0.09 cm<sup>3</sup>/g, respectively, most probably as a result of pore blockage. The main reason for the decrease of the specific surface

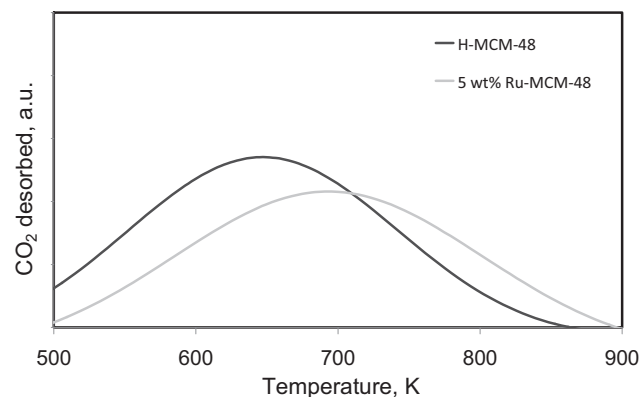


Fig. 3. TPO patterns of the spent MCM-48 and 5 wt% Ru-MCM-48.

area is the blockage of the pores by large hydrocarbon molecules and carbon deposits, suggested by the corresponding decrease of the relative volume of the micropores and mesopores around 2 nm [33].

TPO analysis of the spent catalysts was also conducted to determine the presence of carbon deposits on the mesoporous materials used. During the TPO analysis, carbonaceous deposits on the catalyst surface are oxidized by molecular oxygen resulting in CO<sub>2</sub> signal that can be related to the concentration of the deposits. No CO<sub>2</sub> peaks were detected during the TPO analysis of the fresh catalysts. However, the spent samples of both the MCM-48 and the ruthenium metal modified Ru-MCM-48 were characterized with a markedly significant amount of CO<sub>2</sub> desorbed related to the deposits (Fig. 3). Thus, the TPO results obtained suggest formation of carbon deposits or coke on the catalyst. The non closure of the TOC mass balance in the liquid phase may be at least partially caused by the carbon deposits. Based on the amount of CO<sub>2</sub> released, MCM-48 in the proton form was the catalyst bearing the highest amounts of carbon deposits compared to Ru-MCM-48. Carbon deposits formed during the reaction may also diminish the catalyst activity of the acid sites and ruthenium active metal at prolonged reaction times.

### 3.2. Hydrolytic hydrogenation

Hydrolytic hydrogenation of arabinogalactan was carried out in a batch mode at 20 bar of hydrogen gas and temperature of 458 K. The hydrolysis of hemicellulose over heterogeneous catalysts leads to either poor conversions at low temperatures or to high conversions at higher temperatures, with however, a large spectrum of degradation products. The above mentioned reaction conditions were chosen to evaluate the reaction network for the hydrolytic hydrogenation of the hemicellulose and to facilitate a direct comparison of the hemicellulose with cellulose under similar reaction conditions previously reported in [12]. As already mentioned above, it is generally accepted that hemicelluloses are easier to degrade than cellulose due to their branched and non-crystalline structure. It should also be taken into account that while the hemicelluloses readily dissolve in aqueous solutions, transfer resistance between solid acid catalyst and the insoluble or partially soluble

Table 2  
Brønsted and Lewis acidities of the fresh catalyst.

Catalyst	Brønsted acid sites (μmol/g)			Lewis acid sites (μmol/g)		
	523 K	623 K	723 K	523 K	623 K	723 K
MCM-48	59	18	2	63	25	7
Ru-MCM-48	58	7	1	69	10	1

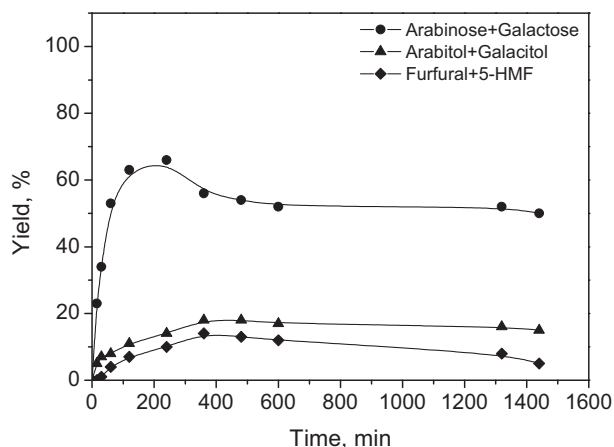


Fig. 4. Product yields for the non-catalytic hydrolytic hydrogenation of arabinogalactan at 458 K and 20 bar hydrogen pressure.

cellulose in water will restrict the catalytic activity. The mechanism which is widely accepted for the acid catalyzed hydrolysis of the hemicellulose in water is based on the protonation of the glycosidic oxygen resulting in the cleavage of the glycosidic bond between the sugar units and formation of the monosaccharides [10]. The hydrolysis of the hemicellulose is then proceeded by the hydrogenation of the simple sugars over the active metal sites on the solid catalyst to polyols. At the same time, dehydration of the sugars to furan compounds may also occur in the acidic media. Hence, the hydrolytic hydrogenation of the hemicellulose proceeds via several routes depending on the nature of the catalytic material used.

A non-catalytic experiment was conducted to determine the background activity in the absence of a catalyst. The experiment was conducted at 458 K and 20 bar of hydrogen pressure. The main products detected were arabinose, galactose, arabitol, galacitol, furfural and 5-hydroxymethylfurfural. The product yields as a function of time are shown in Fig. 4. It can be seen that the hydrolysis products were released in significant amounts with a maximum yield of 65% arabinose and galactose after 240 min, being a substantial amount considering the fact that the reaction was conducted in the absence of any catalyst. This phenomenon can be explained probably by the in situ produced  $H^+$  ions in the hot compressed water. The  $pK_w$  value of water at 458 K has been reported to be 11.4 compared to the well known value of 14 at 298 K [34]. Higher temperatures have an advantage to accelerate the hydrolysis of arabinogalactan in a “quasi” non-catalyzed reaction due to the  $H_3O^+$  which might act as a catalyst. Therefore, even though the action of the solid acid sites was excluded, the partial hydrolysis of arabinogalactan took place and the products resulting from the acid catalyzed reactions were observed. With increasing reaction times, the yields of arabinose and galactose decreased implying that they undergo further degradation. Sugar alcohols and furan compounds were also detected in the liquid phase although in small amounts. Several by-products were detected in low quantities, ranging from one to five carbon atoms originating from further degradation of the sugars and furan compounds similar to results previously reported in the literature [35,36] and also obtained over MCM-48 (Section 3.3). The mass balance closure of the liquid phase products detected by both the HPLC and analyzed by total organic carbon was more than 80% after 1440 min. This incomplete mass balance was due to the formation of gaseous by-products, carbon and coke deposits in the reactor. The color of the reaction mixture turned from a clear solution to brownish color after the experiment pointing out that further degradation occurred. It has also been reported in Ref. [12] that the unstable sugars degrade (caramelize) under high thermal treatments.

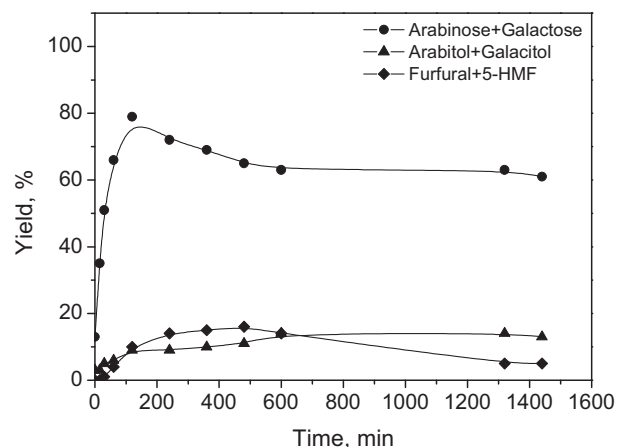


Fig. 5. Product yields for the hydrolytic hydrogenation of arabinogalactan over MCM-48 at 458 K and 20 bar hydrogen pressure.

### 3.3. Comparison of H-MCM-48 and Ru-MCM-48

The hydrolytic hydrogenation of arabinogalactan was performed over MCM-48 and the metal modified Ru-MCM-48 mesoporous material to evaluate the influence of the catalytic materials in the reaction. The MCM-48 support material has BAS and they possess similar acidic properties compared to mineral acid catalysts such as HCl and  $H_2SO_4$ . Owing to the mesoporous crystalline structure, MCM-48 displays mild acidity to facilitate the hydrolysis of the hemicellulose and at the same time suppresses the extent of the undesired degradation reactions. The Brønsted acidity required for the hydrolysis of the glycosidic bonds of the bulk arabinogalactan is provided by the external surface acid sites of the mesoporous material. It is postulated that the hemicelluloses hydrolyze on the external acid sites [13], and then the oligomers are formed which can enter the pores and interact with the internal acid sites to yield the monomers, arabinose and galactose. The sugars might then undergo dehydration to give furan compounds, furfural and 5-hydroxymethylfurfural on these internal sites. The product yields obtained with MCM-48 as a function of time are shown in Fig. 5. The products identified were similar to the non-catalytic experiment but the distribution and the time at which the maximum sugar yields were reached was achieved after 120 min. The rate of arabinogalactan conversion was twofold and subsequently the time to reach the maximum sugar yields was just half when catalyzed by MCM-48 in comparison with a non-catalytic experiment. A complete transformation of the hemicellulose was achieved in both cases after 1440 min. The results suggest that the presence of MCM-48 enhances the hydrolysis of arabinogalactan.

During the initial stages of the reaction, the main products formed were the monosaccharides, arabinose and galactose. There was a significant increase in the amount of monosaccharide yields reaching a maximum value close to 80% after 120 min. The high catalyst acidity of the mesoporous MCM-48 material is understood to be the reason for the faster rates of arabinose and galactose formation. The amount of the sugars, however, decreased at prolonged reaction times. This was at the expense of the consecutive transformation of the sugars to furan compounds, furfural and 5-hydroxymethylfurfural from arabinose and galactose, respectively. The sugar alcohols were also formed although in lower quantities compared to furfurals. It is reasonable to suggest that dehydration of the sugars is favored by the BAS of the catalyst. Dehydration of pentoses and hexoses over zeolites and mesoporous materials in the temperature range of 370–470 K has been reported in the literature [2]. The acidity of the MCM-48 can also be linked to the further degradation of these compounds to low molecular weight

by-products and coke. The total amount of furan compounds was noticed to be decreasing after 480 min. Furthermore, the color of the reaction mixture turned from a light and clear solution to a dark brown solution after the experiment suggesting that further degradation of the products occurred.

Considering the hydrogenation step as the main process which consumes hydrogen, the total hydrogen consumed was 0.65 mmol. The total pressure in the semi-batch reactor remained constant at 20 bars during the reaction, which implies that the amount of hydrogen in the liquid phase was 26 mmol taking into account the Henry constant for water at these conditions. The excess amount ensures that hydrogen was not limiting the evolution of the reactions and, consequently, the final product yields were determined by the amount and strength of the active centers of the catalyst following the mechanism of the reaction.

Using the GC–MS, several by-products, mainly low molecular weight alcohols and acid compounds were identified, ranging from one to five carbon atoms, according to different degradation steps. Some of the by-products detected were glycerol, glycol, propylene glycol acetic acid, lactic acid, hydroxypropanoic acid, hydroxybutyric acid and dihydroxypentanoic acid. The total concentration of the by-products detected in the liquid phase was never higher than 5%. The low concentration and the high variety of the isomers of these by-products make it difficult to follow the evolution of each component. The acidic products resulted in the drop of the pH of the filtered reaction mixture from close to the initial neutral to 4.38 after 1440 min reaction time. The mass balance closure analyzed by total organic carbon after 1440 min was 75%, indicating a slightly lower TOC than in the case of the non-catalytic reaction. Higher acidity promoted hydrolysis, dehydration and also further degradation processes, forming gaseous products (mainly CO<sub>2</sub>) and carbon deposits thus explaining this lower mass balance closure.

To demonstrate the bi-functional properties of the catalytic material, the hydrolytic hydrogenation of arabinogalactan was conducted over the ruthenium metal modified 5 wt% Ru–MCM-48

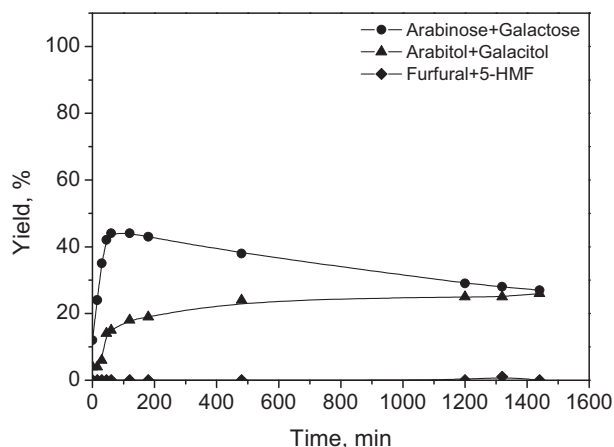
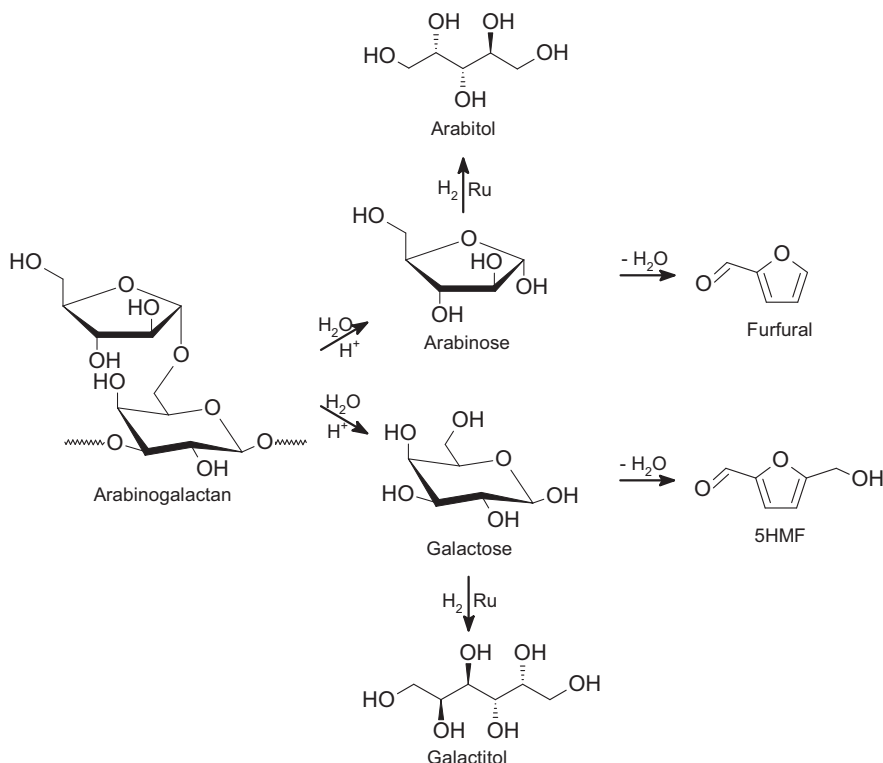


**Fig. 6.** Product yields for the hydrolytic hydrogenation of arabinogalactan over 5 wt% Ru–MCM-48 at 458 K and 20 bar hydrogen pressure.

(Fig. 6). The hemicellulose, arabinogalactan was hydrolyzed to arabinose and galactose, and the sugars were subsequently hydrogenated to sugar alcohols, arabitol and galacitol, respectively. The hydrolysis of the hemicellulose can be ascribed to the BAS of the mesoporous material, while the hydrogenation of the sugars occurs on the active ruthenium metal sites. The maximum sugar yields obtained by the metal modified mesoporous material were, as expected, not as high as with MCM-48 due to the consecutive reactions taking place. The sugar yields were 45% after 120 min, and thereafter a decline in the amount of arabinose and galactose in the reaction mixture was observed. This was attributed to the subsequent hydrogenation of the sugars to polyols which were in this case, obtained in significantly higher yields compared to both the non-catalytic and the MCM-48 catalyzed reactions. The polyols, arabitol and galacitol were obtained in almost 30%



**Scheme 1.** Reaction network for the hydrolytic hydrogenation of arabinogalactan.

yield after 1440 min. Ruthenium metal demonstrated a high catalytic activity in the sugar hydrogenation, manifested by the high selectivity towards the polyols. In a separate hydrogenation experiment with either pure arabinose or galactose, it was confirmed that ruthenium catalyst was an effective catalyst for the production of arabitol and galactitol, respectively. Virtually no furan compounds were detected in the reaction mixture. The presence of the active metal in the structure of MCM-48 leads to the hydrogenation of the sugars into arabitol and galactitol rather than being dehydrated into furfural and 5-hydroxymethylfurfural. The product yield profiles obtained in Fig. 6 demonstrated an increase in the arabitol and galactitol yields and, most interestingly, a total suppression of the furfural and 5-hydroxymethylfurfural formation which was a competitive route. The sugar alcohols selectivity evolved from 16.5% obtained with MCM-48 to 48% obtained with the metal modified Ru–MCM-48 catalyst. The introduction of the ruthenium metal function of the catalyst, combined with the reductive atmosphere, hydrogen, seems to be a justifiable tool to make the reaction more selective towards the more stable sugar alcohols as also reported in Ref. [10]. In this case, the amount of hydrogen consumed was 0.36 mmol, and due to the excess of hydrogen in the reaction mixture, it can be concluded that its amount was not limiting the progress of the reaction. Degradation by-products similar to previously mentioned and total organic carbon around 75% was observed for ruthenium metal modified catalyzed reaction. However, in contrast to the MCM-48 catalyzed reaction, the metal modified mesoporous Ru–MCM-48 catalyzed reaction had a final pH 6.12 of the filtered solution after 1440 min. This indicates a lower proportion of the acidic by-products formed in the presence of 5 wt% Ru–MCM-48. A combination of the by-products detected and the TPO profiles, suggests that the low mass balance closure was mainly due to the formation of gaseous products as well as carbon and coke deposits from the degradation products.

### 3.4. Reaction network

The reaction pathway for the hydrolytic hydrogenation of arabinogalactan proposed based on the experimental data is shown in Scheme 1. The hydrolytic hydrogenation of arabinogalactan proceeds via two reaction routes, hydrolysis of the hemicellulose over the acid sites leading to the formation of the simple sugars, arabinose and galactose. In the presence of ruthenium metal in the catalytic material, the monosaccharides are hydrogenated into arabitol and galactitol. The presence of the ruthenium on the support material can therefore be crucial on the product selectivity. If hydrolysis is the rate limiting step in the reaction system, the sugars formed will be hydrogenated into sugar alcohols, whereas if hydrogenation is the rate limiting step, the sugars will be dehydrated into furfurals. The large amounts of furfural and 5-hydroxymethylfurfural indicate that the hydrogenation is the rate limiting step. Decarbonylation of 5-hydroxymethylfurfural can furthermore take place producing furfural as reported in Ref. [37]. This implies that furfural can originate from both arabinose and galactose. Furthermore, low molecular weight degradation products of the sugars and furfurals may appear, or coke that may be deposited on the surface of the catalyst, can be formed especially over MCM-48. The proposed reaction scheme is somewhat similar to the one previously reported for the hydrolytic hydrogenation of bleached birch kraft pulp [12].

## 4. Conclusions

The hydrolytic hydrogenation of a hemicellulose, arabinogalactan, was carried out over MCM-48 and the metal modified mesoporous Ru–MCM-48 materials. The ordered mesoporous

MCM-48 was synthesized, incorporated with ruthenium, characterized by several techniques and evaluated in the title reaction. The transformation of the hemicellulose comprises of the hydrolysis of arabinogalactan to L-arabinose and D-galactose followed by the subsequent hydrogenation to arabitol and galactitol or dehydration of the monomers to furfural and 5-hydroxymethylfurfural. Although the hydrolysis of the hemicellulose can take place due to the in situ produced H<sup>+</sup> ions in the hot compressed water, the acidity of the mesoporous MCM-48 was demonstrated to enhance the hydrolysis. Dehydration of the sugars to furfural and 5-hydroxymethylfurfural may occur due to the acidic nature of the catalyst. The hydrogenation of the monosaccharides was ascribed to the presence of ruthenium in the metal modified catalysts. The sugar alcohols were obtained selectively over Ru–MCM-48 catalyst. The balance between the two catalytic functions is necessary for the overall productivity depending on the desired product. The unique properties of the heterogeneous mesoporous materials give them an exceptional application in one-pot transformation of hemicelluloses as bi-functional catalysts containing an acid function and an active metal.

## Acknowledgments

This work is part of the activities at the Åbo Akademi University, Process Chemistry Centre within the Finnish Centre of Excellence Program (2000–2011) appointed by the Academy of Finland. L. Faba thanks the Government of the Principality of Asturias for a Ph.D. fellowship (Severo Ochoa Program).

## References

- [1] P. Mäki-Arvela, B. Holmbom, T. Salmi, D. Yu Murzin, *Catal. Rev.* 49 (2007) 197–340.
- [2] J.N. Chheda, G.W. Huber, J.A. Dumesic, *Angew. Chem. Int. Ed.* 46 (2007) 7164–7183.
- [3] E. Sjöström, *Wood Chemistry – Fundamentals and Applications*, 2nd ed., Academic Press, San Diego, 1993.
- [4] S. Willför, R. Sjöholm, C. Laine, B. Holmbom, *Wood Sci. Technol.* 36 (2002) 101–110.
- [5] S. Willför, B. Holmbom, *Wood Sci. Technol.* 38 (2004) 173–179.
- [6] V.A. Babkin, Yu A. Malkov, E.N. Medvedeva, N.N. Trofimova, N.V. Ivanova, *Russian Chem. J.* (2011) 10–16.
- [7] R. Rinaldi, F. Schüth, *ChemSusChem* 2 (2009) 1096–1107.
- [8] B.T. Kusema, C. Xu, P. Mäki-Arvela, S. Willför, B. Holmbom, T. Salmi, D.Yu. Murzin, *Int. J. Chem. Reactor Eng.* 8 (A44) (2010) 1–16.
- [9] B.T. Kusema, G. Hilppmann, P. Mäki-Arvela, S. Willför, B. Holmbom, T. Salmi, D. Yu Murzin, *Catal. Lett.* 141 (2011) 408–412.
- [10] P. Mäki-Arvela, T. Salmi, B. Holmbom, S. Willför, D. Yu Murzin, *Chem. Rev.* 111 (2011) 5638–5666.
- [11] A. Fukuoka, P.L. Dhepe, *Angew. Chem. Int. Ed.* 45 (2006) 5161–5163.
- [12] M. Kälndström, N. Kumar, D. Yu Murzin, *Catal. Today* 167 (2011) 91–95.
- [13] P.L. Dhepe, R. Sahu, *Green Chem.* 12 (2010) 2153–2156.
- [14] P.M. Collins, R.J. Ferrier, *Monosaccharides: Their Chemistry and Their Roles in Natural Products*, John Wiley & Sons Ltd, England, 1995.
- [15] L. Faba, E. Díaz, S. Ordóñez, *Catal. Today* 164 (2010) 451–456.
- [16] S. Ordóñez, E. Díaz, M. León, L. Faba, *Catal. Today* 167 (2011) 71–76.
- [17] J.S. Beck, J.C. Vartuli, W.J. Roth, M.E. Leonowicz, C.T. Kresge, K.D. Schmitt, C.T.W. Chu, D.H. Olson, E.W. Sheppard, S.B. McCullen, J.B. Higgins, J.L. Schlenker, *J. Am. Ceram. Soc.* 114 (1992) 10834–10843.
- [18] C.T. Kresge, M.E. Leonowicz, W.J. Roth, J.C. Vartuli, J.S. Beck, *Nature* 359 (1992) 710–712.
- [19] Ch. Baerlocher, L.B. McCusker, D.H. Olson, *Atlas of Zeolite Framework Types*, 6th ed., Elsevier Science, Amsterdam, 2007.
- [20] S.B. Pu, J.B. Kim, M. Seno, T. Inui, *Microporous Mater.* 10 (1997) 25–33.
- [21] C. Luo, S. Wang, H.C. Liu, *Angew. Chem. Int. Ed.* 46 (2007) 7636–7639.
- [22] D. Trong On, D. Desplandier-Giscard, C. Danumah, S. Kaliaguine, *Appl. Catal. A: Gen.* 222 (2001) 299–357.
- [23] X. Luo, Z. Wang, L. Chen, X. Wang, B. Wu, *Catal. Lett.* 132 (2009) 450–453.
- [24] M. Hartmann, C. Bischof, Z. Luan, L. Kevan, *Microporous Mesoporous Mater.* 44–45 (2001) 385–394.
- [25] C.D. Baertsch, M.A. Schmidt, K.F. Jensen, *Chem. Commun.* (2004) 2610–2611.
- [26] A.M. Karim, V. Pransad, G. Mpourmpakis, W.W. Lonergan, A.I. Frenkel, J.G. Chen, D.G. Vlachos, *J. Am. Ceram. Soc.* 131 (2009) 12230–12239.
- [27] C.A. Emeis, *J. Catal.* 143 (1993) 347–354.

- [28] F. Bertaud, A. Sundberg, B. Holmbom, *Carbohydr. Polym.* 48 (2002) 319–324.
- [29] M.A. Cambor, A. Corma, S. Valencia, *Microporous Mesoporous Mater.* 25 (1998) 59–74.
- [30] L.A. Solovoyov, O.V. Belousov, R.E. Dinnebier, A.N. Shmakov, S.D. Kirik, *J. Phys. Chem. B* 109 (2005) 3233–3237.
- [31] F. Wei, Z. Liu, J. Lu, *Microporous Mesoporous Mater.* 131 (2010) 224–229.
- [32] D. Kubička, N. Kumar, T. Venäläinen, H. Karhu, I. Kubičková, H. Österholm, D.Yu. Murzin, *J. Phys. Chem. B* 110 (2006) 4937–4946.
- [33] M. Guisnet, Carbonaceous deposits, in: G. Ertl, H. Knözinger, J. Weitkamp (Eds.), *Handbook of Heterogeneous Catalysis*, vol. 2, Wiley-VCH, New York, 1997, pp. 626–632.
- [34] W.L. Marshall, E.U. Franck, *J. Phys. Chem. Ref. Data* 10 (2) (1981) 295–304.
- [35] C. Chang, X. Ma, P. Peilin, *J. Chem. Eng.* 17 (2009) 835–839.
- [36] I.T. Horváth, H. Mehdí, V. Fábos, L. Boda, L.T. Mika, *Green Chem.* 10 (2008) 238–242.
- [37] E.J. Shin, M.R. Nimlos, R.J. Evans, *Fuel* 80 (2001) 1697–1709.